Biochimica et Biophysica Acta 1853 (2015) 940–952

Contents lists available at ScienceDirect

Biochimica et Biophysica Acta

journal homepage: www.elsevier.com/locate/bbamcr

Fascin actin bundling controls podosome turnover and disassembly while cortactin is involved in podosome assembly by its SH3 domain in THP-1 macrophages and dendritic cells

Isabel Van Audenhove, Nincy Debeuf, Ciska Boucherie, Jan Gettemans *

Department of Biochemistry, Faculty of Medicine and Health Sciences, Ghent University, Albert Baertsoenkaai 3, B-9000 Ghent, Belgium

ARTICLE INFO

Article history:
Received 19 September 2014
Received in revised form 11 December 2014
Accepted 8 January 2015
Available online 16 January 2015

Keywords:
Podosome
Fascin
Cortactin
Nanobody
Actin dynamics

ABSTRACT

Podosomes are dynamic degrading devices present in myeloid cells among other cell types. They consist of an actin core with associated regulators, surrounded by an adhesive ring. Both fascin and cortactin are known constituents but the role of fascin actin bundling is still unclear and cortactin research rather focuses on its homologue hematopoietic lineage cell-specific protein-1 (HS1). A fascin nanobody (FASNb5) that inhibits actin bundling and a cortactin nanobody (CORNb2) specifically targeting its Src-homology 3 (SH3) domain were used as unique tools to study the function of these regulators in podosome dynamics in both THP-1 macrophages and dendritic cells (DC). Upon intracellular FASNb5 expression, the few podosomes present were aberrantly stable, long-living and large, suggesting a role for fascin actin bundling in podosome turnover and disassembly. Fascin modulates this by balancing the equilibrium between branched and bundled actin networks. In the presence of CORNb2, the few podosomes formed show disrupted structures but their dynamics were unaffected. This suggests a role of the cortactin SH3 domain in podosome assembly. Remarkably, both nanobody-induced podosome-losses were compensated for by focal adhesion structures. Furthermore, matrix degradation capacities were altered and migratory phenotypes were lost. In conclusion, the cortactin SH3 domain contributes to podosome assembly while fascin actin bundling is a master regulator of podosome disassembly in THP-1 macrophages and DC.

1. Introduction

Podosomes are cell-matrix contacts present at the ventral side of myeloid, smooth muscle and endothelial cells. They consist of an F-actin core with actin regulators such as Wiskott–Aldrich syndrome protein (WASP) and actin-related protein (Arp2/3), and an adhesive ring rich in vinculin and talin, among others [1]. Podosomes differ from invadopodia, their counterparts in cancer cells, in lifetime, protrusive dimensions and actin network arrangement [2]. Functionally, podosomes are involved in adhesion [1], matrix degradation [3], mechanosensing [4] and directional migration [5]. Furthermore, they contribute to invasive cell migration in vivo [6,7]. Pathologically, podosome loss is linked to defects in immune cell migration in patients carrying WASP mutations [8] and to defects in bone resorption by failure of osteoclast sealing zone formation [9].

The actin-bundling protein fascin is aberrantly expressed in numerous cancer types and is considered a metastatic marker and therapeutic target [10]. Fascin has been detected in invadopodia where it stabilizes actin and contributes to turnover, matrix degradation and invasion [11,12]. Podosomes also contain fascin, although its precise function remains unclear as both an assembling and disassembling role were previously reported [13,14]. In dendritic cells (DC), fascin levels are induced upon maturation [15] thereby contributing to migration [14] and antigen presentation [16].

Cortactin and hematopoietic lineage cell-specific protein-1 (HS1) are multidomain proteins consisting of an NTA acidic Arp2/3-binding domain, actin binding repeats, a helical domain, a proline-rich regulatory domain and an Src-homology 3 (SH3) domain interacting with (neural)-Wiskott Aldrich syndrome protein (N)-WASP, WASP-interacting protein (WIP) or dynaminII among others [17]. Cortactin is upregulated in many cancers and contributes to invadopodium formation, matrix degradation and cell

Abbreviations: Arp, actin-related protein; CORNb, anti-cortactin nanobody; DC, dendritic cells; EGFP, enhanced green fluorescent protein; FASNb, anti-fascin nanobody; GELNb, anti-gelsolin nanobody; GM-CSF, granulocyte macrophage colony-stimulating factor; HS1, hematopoietic lineage cell-specific protein-1; IL, interleukin; Nb, nanobody; LPS, lipopolysaccharide; N-WASP, neural Wiskott–Aldrich syndrome protein; PBMC, peripheral blood mononuclear cells; PMA, phorbol-12-myristate-13-acetate; SH3, Src-homology 3; VCA, verprolin, cofilin, acidic homology; WASP, Wiskott–Aldrich syndrome protein; WIP, WASP-interacting protein

* Corresponding author at: Department of Biochemistry, Albert Baertsoenkaai 3, B-9000 Ghent, Belgium. Tel.: +32 9 2649340; fax: +32 9 2649490.
E-mail address: jan.gettemans@ugent.be (J. Gettemans).

http://dx.doi.org/10.1016/j.bbamcr.2015.01.003
0167-4889/

invasion, in part through its SH3 domain [18,19,12]. HS1 on the other hand is expressed in hematopoietic cells where it regulates lamellipodial dynamics, directional migration, antigen uptake and presentation [20,21]. However, the role of cortactin next to HS1 in macrophages or DC is still unclear.

Nanobodies represent the antigen-binding fragments of *Camelid* heavy-chain antibodies [22]. Due to their size (15 kDa), stability, specificity and affinity they have become an emerging tool in research, diagnostics and therapeutics [23]. Their target-modulating activity in combination with their intracellular functionality makes them useful for knockout of endogenous protein functions or domains [24–27,12].

In this study we applied nanobodies against fascin and cortactin to gain insight into their specific contributions in podosome formation, dynamics and function. The fascin nanobody (FASNb5) inhibits actin bundling activity. The cortactin-targeting nanobody (CORNb2) binds the SH3 domain but does not cross-react with its homologue HS1 [12]. With these tools, we unravel a podosome disassembling role dependent on fascin actin bundling activity and an assembling role relying on the cortactin SH3 domain in THP-1 macrophages and DC. Fascin activity modifies the network from branched towards bundled actin filaments resulting in podosome turnover, disassembly and recycling of constituents. The cortactin SH3 domain on the other hand contributes to proper podosome assembly without affecting dynamics. Both functional knockouts lead to a switch from podosomes to focal adhesions and eventually affect the degrading and migratory phenotype.

2. Material and methods

2.1. Antibodies and reagents

Rabbit polyclonal anti-fascin (FSCN1), mouse monoclonal anti-vinculin (hVIN-1) and V5-agarose (V5–10) were obtained from Sigma (St. Louis, MO, USA). Mouse monoclonal anti-fascin (55K-2) and rabbit polyclonal anti-Arp2 were obtained from Abcam (Cambridge, UK). Rabbit polyclonal anti-GFP, rabbit polyclonal anti-cortactin (H-222) and rabbit monoclonal anti-HS1 (D83A8) were obtained from Cell Signaling (Danvers, MA, USA). Mouse monoclonal anti-cortactin was obtained from Millipore (Watford, UK). Alexa Fluor-labeled secondary goat anti-rabbit or anti-mouse IgG antibodies were obtained from Molecular Probes (Eugene, OR, USA). Mouse monoclonal anti-V5 antibody and Alexa Fluor 594-labeled phalloidin were purchased from Invitrogen (Merelbeke, Belgium). Acti-stain 670 phalloidin was purchased from Cytoskeleton (Denver, CO, USA). Protein G Sepharose was obtained from GE Healthcare (Little Chalfont, UK). Cortactin and fascin cDNA were obtained from Origene (Rockville, MD, USA).

2.2. Generation of nanobodies, cDNA cloning and recombinant production

Fascin and cortactin nanobodies were obtained in collaboration with the VIB nanobody service facility and cloned and produced as described earlier [12].

2.3. Cell culture, transduction and transfection

THP-1 monocytic cells (ATCC TIB-202™) and primary DC were maintained at 37 °C in a humified 5% CO2 incubator and grown in RPMI. MDA-MB-231 cells were grown in DMEM and PC-3 cells in RPMI, both at 10% CO_2. All media were supplemented with 10% FBS (heat-inactivated for DC), 100 μg/mL streptomycin and 100 IU/mL penicillin. For THP-1 cells, also 0.05 mM β-mercaptoethanol was supplemented. Cell culture media were obtained from Gibco Life Technologies (Grand Island, NY, USA). Differentiation of THP-1 cells into macrophages was achieved by stimulation with 350 nM phorbol 12-myristate 13-acetate (PMA) for 2–4 days. Stable and inducible expression of EGFP-tagged (enhanced green fluorescent protein) nanobodies in THP-1 cells was achieved by the Lenti-X Tet-On Advanced system of Clontech (Mountain View, CA, USA) as described earlier [24,12]. Expression was induced with 500 ng/mL doxycycline for 24–48 h. Cells were additionally transduced with LifeAct–Cherry for live cell imaging. For DC generation, human peripheral blood mononuclear cells (PBMC) were isolated by Lymphoprep density centrifugation (Stemcell technologies, Grenoble, France) from whole blood samples of healthy donors with informed consent as approved by the local ethical committee (EC UZGhent 2013/467). Adhesion selection was performed to enrich for monocytes and differentiation into DC was induced by addition of 20 ng/mL interleukin-4 (IL-4) and 50 ng/mL granulocyte macrophage colony-stimulating factor (GM-CSF) for 6 days (both from Peprotech, Rocky Hill, NJ, USA). DC were matured by overnight incubation with 0.1 μg/mL lipopolysaccharide (LPS) (Sigma). Transfection of DC was performed with a Neon nucleofection device (Lonza, Cologne, Germany) according to the manufacturer's protocol. Briefly, 700,000 differentiated DC in 100 μL R buffer were added to 3.5 μg DNA and pulsed two times (1000 V, 40 mA).

2.4. Immunostaining and microscopy

Immunostaining was performed as described before [12]. THP-1 cells were seeded onto uncoated coverslips; DC coverslips were coated with Poly-L-lysine (Sigma). Imaging was performed at room temperature with a Zeiss Axiovert 200M Apotome epifluorescence microscope equipped with a cooled CCD Axiocam camera (Zeiss ×63 1.4-NA Oil Plan-Apochromat objective, Carl Zeiss, Oberkochen Germany) and Axiovision 4.5 software (Zeiss) or an Olympus IX81 FluoView 1000 confocal laser scanning microscope (Olympus ×60 1.35-NA Oil UplanSApo objective, Olympus, Tokyo, Japan) with FluoView FV1000 software (Olympus). Z-stacks were taken each 0.5 μm and reconstructed into side views with FluoView FV1000 software (Olympus).

2.5. Live cell imaging of podosomes

THP-1 cells were prepared as described earlier [24]. Time-lapse images were generated using the Olympus confocal microscope (acquisition every 30 s over a period of 30 min in one z plane) and further analyzed with ImageJ. For turnover measurements, podosomes were manually tracked and LifeAct intensity values in the podosome were determined over time. All intensities were normalized to the average LifeAct intensity per podosome over time, which was set as 100%. For lifetime measurements, podosomes were categorized according to the time between first appearance and complete disappearance. For determination of podosome size, podosomes were manually encircled and their area was measured.

2.6. Actin branching assays

Actin branching assays were performed as described earlier [28,29]. For fascin, reaction mixtures contained 2 μM monomeric actin, 60 nM Arp2/3, 100 nM GST–VCA (verprolin, cofilin, acidic homology domain) of WASP, 2 μM fascin and 4 μM FASNb2-His_6-STREP or untagged FASNb5. For cortactin, reaction mixtures contained 2 μM monomeric actin, 8 nM Arp2/3, 30 nM GST–VCA of WASP, 30 nM cortactin and 60 nM GELNb11-V5-His_6 (anti-gelsolin nanobody) [30] or CORNb2-V5-His_6. Nanobodies and their antigens were first pre-incubated for 30 min on ice before addition of the other components. Samples were further diluted in polymerization buffer (10 mM HEPES pH = 7.0, 100 mM KCl, 1 mM $MgCl_2$ and 0.1 mM EDTA, 1 mM DTT) and the reaction was started by addition of 0.2 mM ATP. Polymerization was performed at room temperature

for 3/15 min (fascin) or 10 min/1 h (cortactin). 5% Alexa-Fluor 594-labeled phalloidin was added for 15 min, followed by 20 min incubation of the sample onto poly-L-lysine coated coverslips and mounting. Pictures were manually scored for actin branching after thresholding and particle analysis with ImageJ.

2.7. Statistical analysis

Statistical analysis was performed with SigmaPlot (Systat Software Inc., San Jose, CA, USA) using unpaired student T-tests, one way ANOVA or Mann–Whitney U tests as indicated, both with $p = 0.05$.

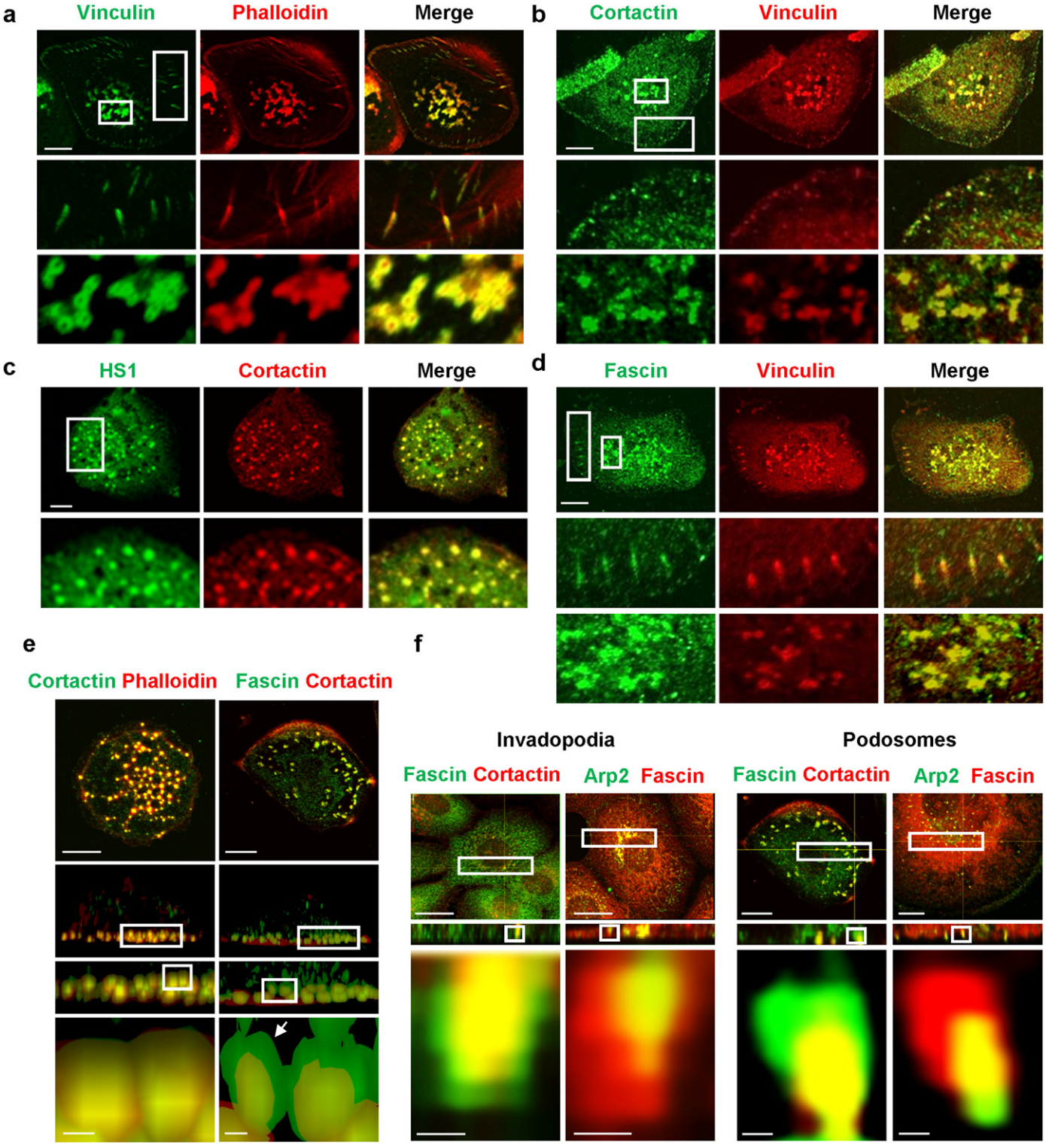

Fig. 1. THP-1 macrophages contain cortactin in the podosome core and fascin in the cap. a. THP-1 macrophages carry both focal adhesions (streak-like pattern) and podosomes (actin dots surrounded by a vinculin ring) as visualized by vinculin and phalloidin. Colocalization of b. cortactin with vinculin, c. cortactin with HS1 and d. fascin with vinculin is shown. Scale bar = 10 μm. e–f. MDA-MB-231 invadopodia or THP-1 podosomes represented as cellular 2D views (upper panels, Scale bar = 10 μm), 3D Z-stack reconstructed side views (middle panels) and zoomed side views (lower panels, Scale bar = 0.5 μm). e. Cortactin and actin colocalize over the podosome core (left), while fascin is additionally present in a cap-like structure (right, white arrows). f. Comparison of colocalization of fascin with cortactin or Arp2 in invadopodia versus podosomes. Fascin localization is completely opposite.

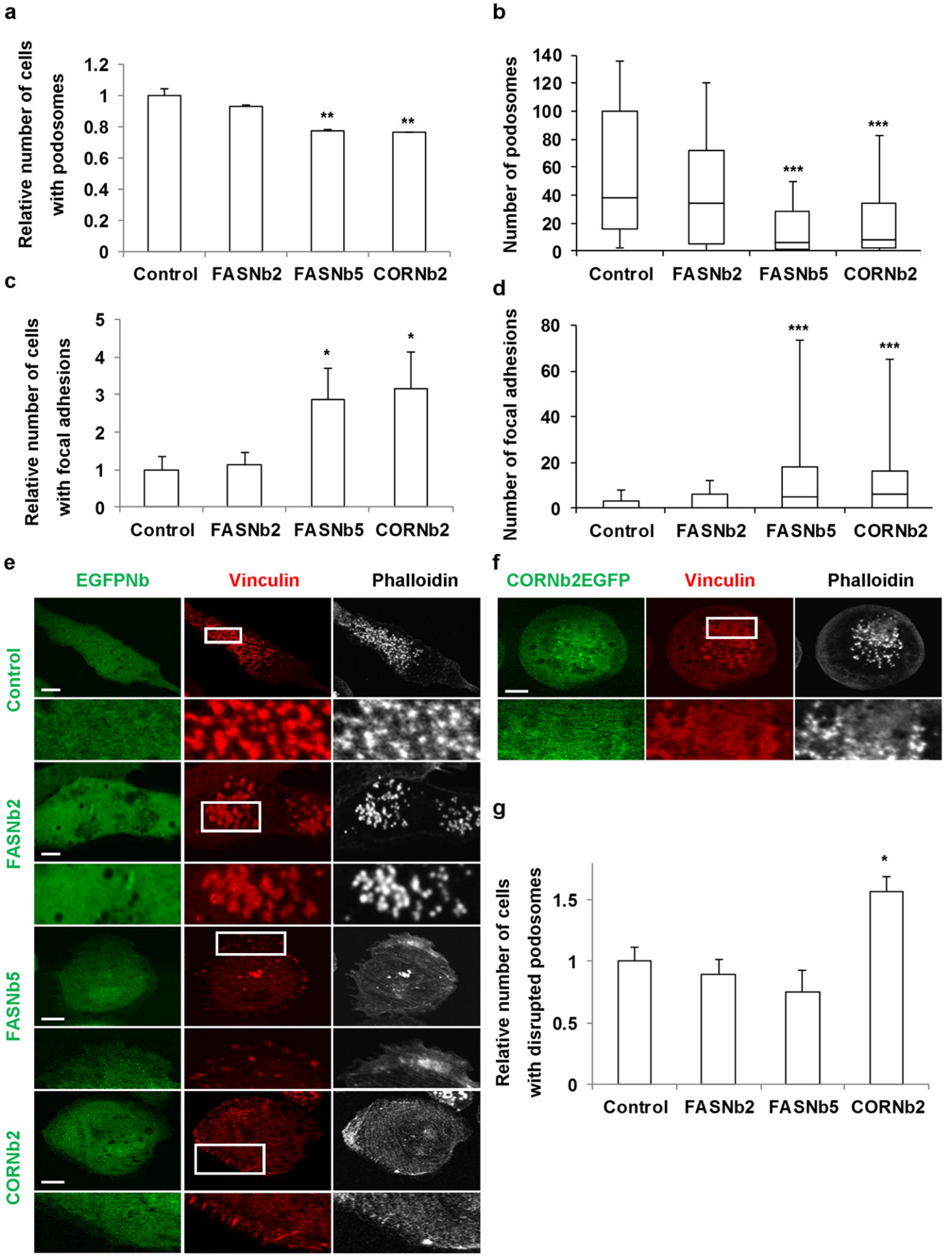
a
Relative number of cells with podosomes
1.2
1
0.8
0.6
0.4
0.2
0
**
**
Control
FASNb2
FASNb5
CORNb2
b
Number of podosomes
140
120
100
80
60
40
20
0
***
***
Control
FASNb2
FASNb5
CORNb2
c
Relative number of cells with focal adhesions
5
4
3
2
1
0
*
*
Control
FASNb2
FASNb5
CORNb2
d
Number of focal adhesions
80
60
40
20
0
***
***
Control
FASNb2
FASNb5
CORNb2
e
EGFPNb
Vinculin
Phalloidin
Control
FASNb2
FASNb5
CORNb2
f
CORNb2EGFP
Vinculin
Phalloidin
g
Relative number of cells with disrupted podosomes
1.5
1
0.5
0
*
Control
FASNb2
FASNb5
CORNb2

3. Results

3.1. THP-1 macrophages carry podosomes with cortactin in the actin-rich core and fascin in the cap structure

To study podosome formation, we used human monocytic leukemia THP-1 cells [31]. Treatment with PMA induces differentiation into macrophages coinciding with the formation of adhesion structures [32]. Vinculin immunofluorescence enables discrimination between streak-like focal adhesion patterns at the end of stress fibers and the ring-like podosome patterns surrounding an actin center (Fig. 1a). Cortactin localizes barely at focal adhesions but is a prominent marker of podosomes (Fig. 1b). Although mostly HS1 is linked to hematopoietic cells [33], THP-1 podosomes contain both cortactin and HS1 (Fig. 1c).

Fascin localizes both at focal adhesions and podosomes (Fig. 1d). In contrast to cortactin, which is present in the actin-rich podosome core, fascin localizes in an upper cap structure (Fig. 1e). This is in striking contrast with its localization in invadopodia, representing similar structures of proteolytic cell invasion typically present in cancer cells. An invadopodium core is composed of branched actin (presence of Arp2 and cortactin) while the protrusive tip is enriched in fascin. In podosomes however, the fascin-rich cap covers the underlying branched actin region (Fig. 1f).

3.2. Disturbance of fascin actin bundling or the cortactin SH3 domain leads to podosome loss and compensation by focal adhesions in THP-1 macrophages

To study fascin and cortactin function, stable inducible cell lines expressing EGFP-tagged fascin or cortactin nanobodies (K_d ~ nM) were generated. EGFP-only expressing cells serve as negative control. Fascin nanobody 5 (FASNb5) specifically inhibits fascin actin bundling both in vitro and intracellular, while fascin nanobody 2 (FASNb2) has no effect [12]. Cortactin nanobody 2 (CORNb2) specifically binds the regulatory SH3-domain of cortactin [12]. Also in the THP-1 cell line, FASNb2/5 bind endogenous fascin and CORNb2 binds endogenous cortactin, but not HS1 (Supplementary Fig. 1a, b). Colocalization studies in LifeAct–Cherry-expressing macrophages further reveal that fascin nanobodies are often not enriched in podosomes, while the cortactin nanobody intensity mostly coincides with actin profiles (Supplementary Fig. 1c).

In the presence of FASNb5 or CORNb2, less cells are capable of forming podosomes (Fig. 2a) and podosome numbers per cell are significantly reduced (Fig. 2b). Note that cell areas were not significantly different (median values: control: 873 μm^2, FASNb5: 951 μm^2, CORNb2: 914 μm^2). Complementary with these observations, more FASNb5 and CORNb2-expressing cells generated focal adhesions (Fig. 2c) and focal adhesion numbers per cell were significantly increased (Fig. 2d, e). When observing podosome patterns in more detail, it further appeared that CORNb2-expressing cells often suffered from disrupted vinculin rings in combination with less discrete, rather 'fuzzy' actin centers (Fig. 2f, g). In conclusion, both FASNb5 and CORNb2 switch the cell adhesion phenotype from podosomes to focal adhesions with CORNb2 additionally disrupting podosome patterns in THP-1 macrophages.

3.3. Fascin actin bundling is essential for podosome turnover and disassembly in THP-1 macrophages

As podosomes are highly dynamic structures [33,3], we performed live cell imaging on LifeAct–Cherry-transduced nanobody-expressing cells. F-actin core turnover occurs several times in individual podosomes of control, FASNb2 and CORNb2-expressing cells (Fig. 3a) [34]. In control cells, podosome actin levels fluctuate from approximately 70% to 130% of the average podosome intensity (which is set at 100%) (Fig. 3b; Videos 1a, 2a). While this is also true for FASNb2 (Videos 1b, 2b) and CORNb2-expressing cells (Videos 1d, 2d), FASNb5 restricts this variation resulting in continuously persisting podosomes (Videos 1c, 2c). Thus, the actin intensity variation in podosomes of FASNb5-expressing cells is significantly limited (Fig. 3c).

We further determined podosome lifetime, which was reported before to be 2–12 min [3]. The most abundant podosome fractions indeed remain maximally 2 min (short-living) or 10 min, while only a slight fraction is really long-living (>30 min) (Fig. 4a). While FASNb2 and CORNb2-dependent distributions are similar to the control, FASNb5 clearly shifts podosome lifetimes, with a significantly decreased short-living podosome fraction and increased long-living podosome fraction. This further results in boosted podosome dimensions (Fig. 4b, c).

In conclusion, inhibiting fascin actin bundling by means of FASNb5 reduces podosome turnover and disassembly and increases podosome sizes in THP-1 macrophages. The cortactin SH3 domain on the other hand does not contribute to dynamics in THP-1 macrophages.

3.4. Fascin actin bundling influences the Arp2/3-mediated actin branching process

To gain more insight into the mechanism by which fascin promotes podosome turnover and disassembly, we performed actin branching assays. In the absence of fascin, Arp2/3 and the WASP-VCA domain mediate branching. Upon fascin addition, actin bundling occurs as showed before by sedimentation assays and electron microscopy [12]. This actin bundling activity significantly inhibits branching (Fig. 5a). FASNb2 has no effect on this phenomenon, while FASNb5 significantly restores the Arp2/3 branching ability. This is in agreement with the inhibitory activity of FASNb5 on fascin actin bundling [12]. For cortactin, its role in branch stabilization was shown before [29]. Indeed, more Arp2/3 and VCA-mediated branches form in the presence of cortactin (Fig. 5b). CORNb2 however has no effect on this stabilizing property.

This observation suggests that FASNb5 counteracts the fascin inhibiting potential on Arp2/3-mediated branching while CORNb2 does not affect cortactin-aided branching activity.

Fig. 2. Both fascin actin bundling and the cortactin SH3 domain contribute to podosome formation and complementary affect focal adhesion formation in THP-1 macrophages. a. Quantification of cells with podosomes represented as normalized means with SEM (n = 3, 100 cells per repeat). Actual percentages: control: 85%, FASNb2: 79%, FASNb5: 66%, CORNb2: 64%. b. Boxplot of podosome numbers (whiskers from 10 to 90%) as determined in at least 100 cells obtained over 3 independent experiments. c. Quantification of cells with focal adhesions represented as normalized means with SEM (n = 3, 100 cells per repeat). Actual percentages: control: 8%, FASNb2: 9%, FASNb5: 23%, CORNb2: 25%. d. Boxplot of focal adhesion numbers (whiskers from 10 to 90%) as determined in at least 100 cells obtained over 3 independent experiments. e. Representative pictures of THP-1 macrophages expressing EGFP (control) or EGFP-tagged nanobodies and visualized with vinculin and phalloidin as used for the quantifications in a–d. Podosomes can be distinguished from focal adhesions by their specific immunofluorescence patterns as shown in Fig. 1a. Control and FASNb2-expressing cells mainly carry podosomes, while more FASNb5 and CORNb2-expressing cells are devoid of podosomes and form focal adhesions instead. Scale bar = 10 μm. f. Representative picture of a CORNb2-expressing cell with a disrupted podosome pattern characterized by disturbed vinculin rings and 'fuzzy' actin centers visualized by phalloidin. Scale bar = 10 μm. g. Quantification of cells with disrupted podosomes as shown in f represented as normalized means with SEM (n = 3, 100 cells per repeat). Actual percentages: control: 13%, FASNb2: 12%, FASNb5: 10%, CORNb2: 20%. P-values were determined with b and d Mann–Whitney U or a, c, and g Student T-tests (* $p < 0.05$, ** $p < 0.01$, *** $p < 0.001$).

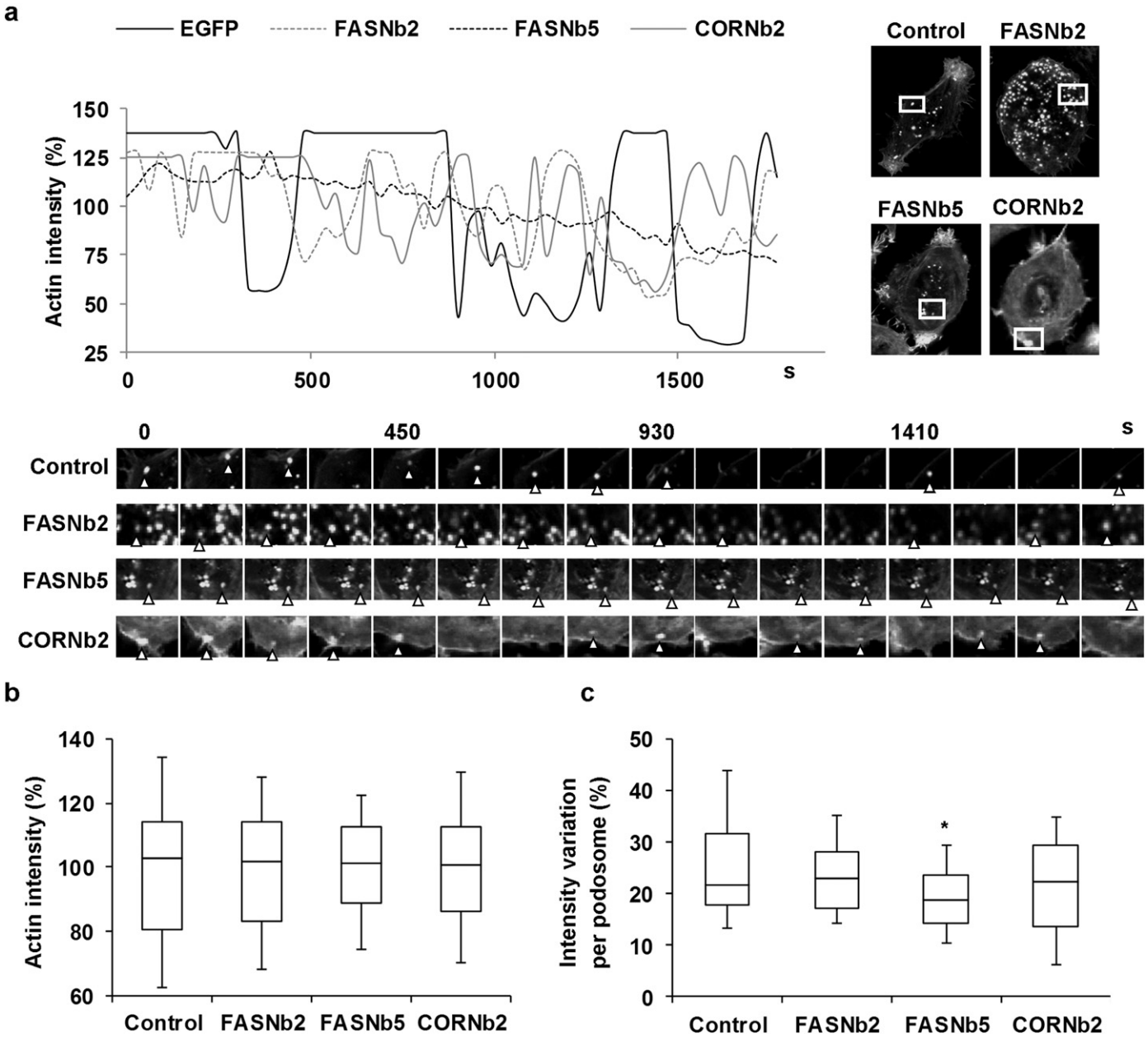

Fig. 3. Fascin actin bundling is crucial for podosome turnover in THP-1 macrophages. Turnover was studied by live cell imaging of LifeAct and EGFP-tagged nanobody-expressing THP-1 cells and further analyzed with ImageJ. a. Actin turnover of a representative podosome per condition. LifeAct (actin) intensity at a podosome was determined each 30 s during 30 min with ImageJ and plotted in function of time. Values were normalized to the average actin intensity per podosome over the time course, which was set as 100%. Intensity peaks higher than 100% represent 'presence' or appearance of podosomes, while intensity drops lower than 100% indicate podosome disappearance. Zoomed LifeAct stills of the corresponding analyzed cells on selected time points are displayed in the bottom panels. Arrowheads indicate 'presence' or appearance of podosomes. b. Actin intensity boxplot (whiskers from 10 to 90%) of 34 to 40 podosomes in 21 to 26 cells obtained over 5 independent experiments and analyzed over time as in a. Podosome actin intensity values of all data points (1400–2500 values over 34–40 curves) were combined to represent overall actin intensity variability and thus podosome turnover. c. Boxplot of intensity variations per podosome (whiskers from 10 to 90%). Standard deviations of actin turnover (as represented in a) were determined per podosome/curve (34–40) and used as a measure for intensity variation and thus podosome turnover. P-values were determined with Mann–Whitney U tests (* $p < 0.05$).

3.5. Disrupting fascin actin bundling or the cortactin SH3 domain switches degradation from podosome- to focal adhesion-dependent and affects migratory phenotypes in THP-1 macrophages

As it is assumed that podosomes contribute to proteolytic matrix degradation for invasion [3], we seeded THP-1 macrophages onto a fluorescently labeled gelatin matrix to analyze degradation (Fig. 6a). From this assay, it was clear that especially cells with disrupted vinculin–actin patterns fail in degradation (Fig. 6b). Importantly, this assay further revealed that both podosomes and focal adhesions can execute matrix degradation (Fig. 6c). Most of the podosome-dependent degradation is therefore compensated by focal adhesion-dependent degradation in FASNb5 and CORNb2-expressing cells (Fig. 6d).

To contribute to the immune response, macrophages must develop a migratory phenotype which is characterized by cell elongation, polarization and podosome presence at the leading lamella [35]. In the presence of FASNb5 or CORNb2, fewer cells are elongated and they maintain a round morphology (Fig. 6e, f). In FASNb5-expressing cells we also noticed that podosomes were often homogenously or centrally distributed rather than specifically enriched at the edge of cells (Fig. 6g), which can be linked to podosome immobility through perturbing their dynamics.

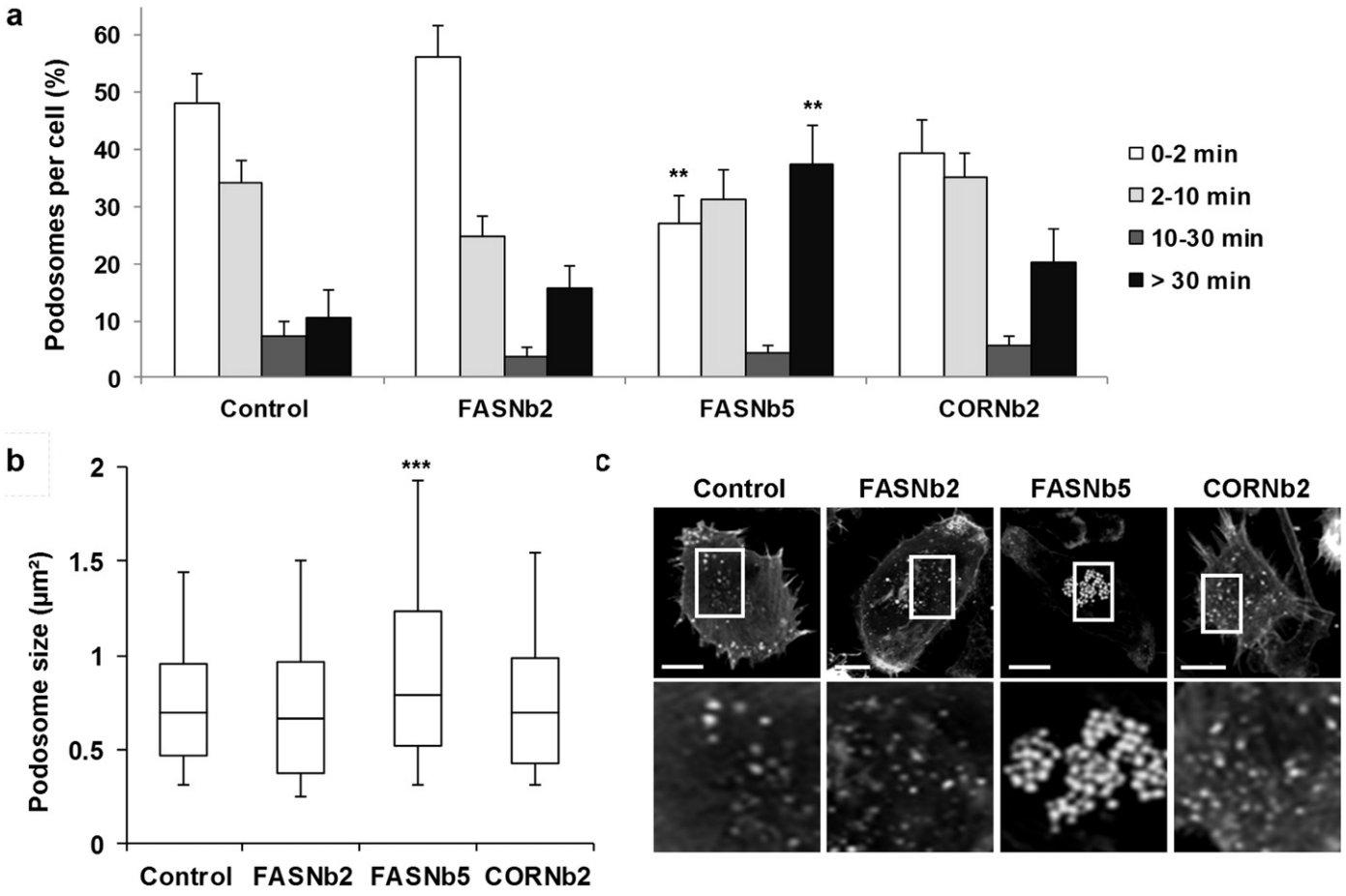

Fig. 4. Fascin actin bundling regulates podosome lifetime and size in THP-1 macrophages. a. Podosome lifetime distributions represented as mean podosome fractions per cell with SEM, determined in 25 cells per condition (328–529 podosomes) obtained over 5 independent experiments. Lifetime was manually determined with ImageJ on the basis of live cell imaging movies (frames each 30 s during 30 min) by tracking frames of podosome appearance and complete disappearance. Long-living podosomes (>30 min) were already present by the start and were still present at the end of imaging without performing fission or fusion events. b. Boxplot of podosomes sizes (whiskers from 10 to 90%) as determined in 25 cells per condition (250 podosomes) obtained over 5 independent experiments. ImageJ was used to compute sizes of 10 podosomes per cell after encircling actin cores. c. Representative LifeAct images of control or nanobody-expressing THP-1 cells, showing differences in podosome size. Scale bar = 10 µm. P-values were determined with Mann–Whitney U-tests (** $p < 0.01$, *** $p < 0.001$).

In summary, the podosome-loss caused by FASNb5 and CORNb2 switches the degradation-type from podosome- to focal adhesion-dependent and impairs the onset of a migratory phenotype in THP-1 macrophages.

3.6. Primary DC also depend on fascin actin bundling and the cortactin SH3 domain for podosome formation and the generation of a migratory phenotype

To check the relevance of our THP-1 macrophage model, we verified our observations in human blood PBMC-derived dendritic cells (DC). Primary DC also form focal adhesions as well as podosomes (Supplementary Fig. **2**a) which contain both cortactin and HS1 and the typical fascin-cap (Supplementary Fig. 2b, c). Western blot analysis confirmed that cortactin levels are lower in immune cells in comparison to cancer cells while the opposite is true for HS1 (Supplementary Fig. 2d). The blot further revealed comparable fascin levels in THP-1 cells and immature DC.

To verify our nanobody-induced effects, immature DC were transfected with V5-tagged intrabodies, with GFPNb as negative control (Fig. 7a). FASNb5 and CORNb2 significantly decreased podosome numbers (Fig. 7b), which coincide with a decline in polarized DC (Fig. 7c). Of note, CORNb2-expressing cells were significantly smaller (median values: control: 345 µm², FASNb5: 359 µm², CORNb2***: 270 µm², *** $p < 0.001$ Mann–Whitney U test). This is due to a lack of spreading capacity on the poly-L-lysine coating used, which will also contribute to the decline in podosome and polarized DC numbers. Indeed, podosome numbers normalized to the cell areas are still significantly but less reduced in the case of CORNb2 (* $p < 0.05$, Mann–Whitney U test).

In conclusion, FASNb5 and CORNb2 also disturb podosome formation in primary DC, which are comparable to THP-1 cells concerning their antigen features.

Furthermore, an interesting feature of primary DC is that upon maturation, achieved by addition of LPS, fascine levels increase four-fold (Supplementary Fig. 2e). Fascin is therefore a useful maturation marker for DC [15]. Immature DC are nicely polarized with podosomes enriched at the front (Fig. 7d). In striking contrast, mature DC with high fascin levels are often devoid of podosomes, rounded and not polarized (Fig. 7e, f). So, also elevated fascin levels are related to podosome loss and a lack of migratory phenotype.

4. Discussion

4.1. Role of fascin actin bundling in podosome dynamics and disassembly

Our experiments with FASNb5 unravel a mechanism as represented in Fig. 8. Podosome building blocks are in a constant equilibrium between Arp2/3-mediated actin branching and fascin-mediated actin bundling. Emphasis is on branching upon assembly, enabling podosome growth. Fascin activity results in loss of branches in the protrusive tip and force generation by bundles on top, permitting turnover and disassembly. This process generates building blocks for new podosomes.

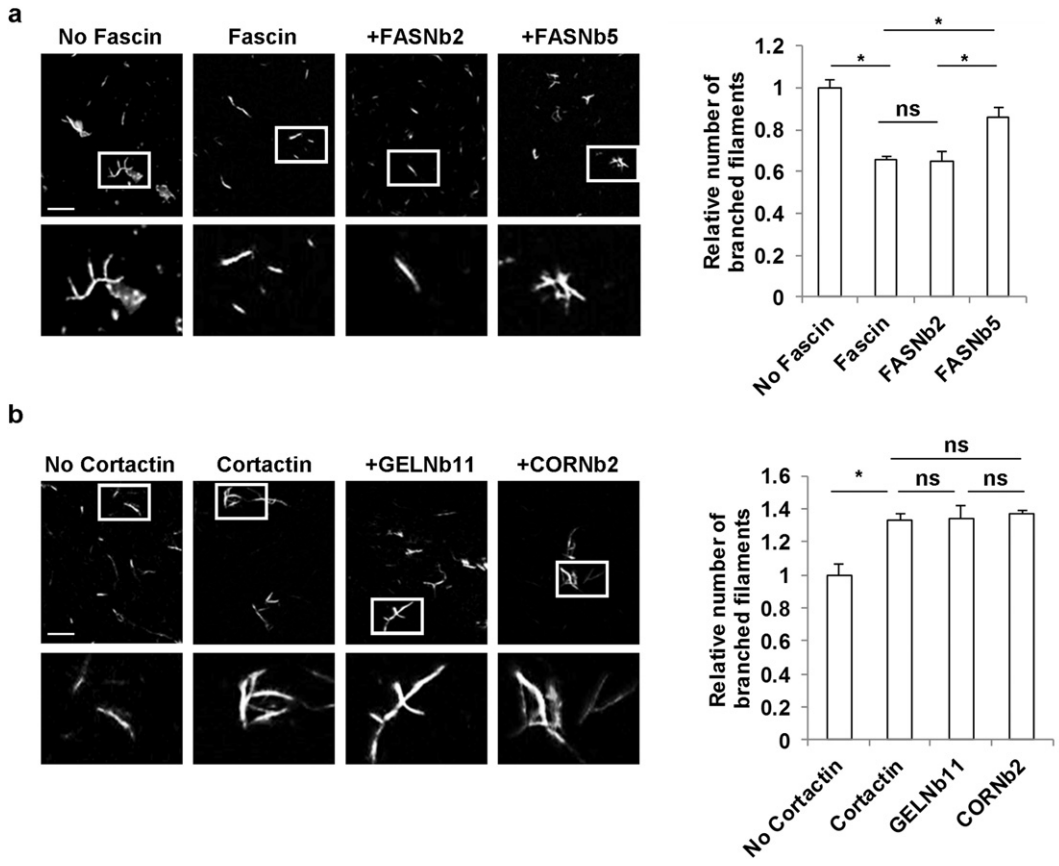

Fig. 5. FASNb5 counteracts fascin actin bundling-mediated inhibition of Arp2/3 branching activity. Actin was allowed to polymerize in the presence of Arp2/3 and the VCA domain of WASP a. with (out) fascin and fascin nanobodies or b. with (out) cortactin and gelsolin/cortactin nanobodies. GELNb11 targets the actin-binding protein gelsolin and is used as a negative control. Representative phalloidin-stained actin filaments after 3 min (fascin) or 10 min (cortactin) polymerization representing the onset of branching are shown in the left panels. Scale bar = 10 μm. The bar charts in the right panels represent normalized means of branched filaments with SEM from 3 independent experiments with 10 replicates each (851–2024 filaments in total). For this quantification, polymerization was performed for 15 min (fascin) or 1 h (cortactin) and 10 random frames were analyzed per experiment. Filaments were manually scored for branching in ImageJ after thresholding (pixels 50–255) and particle selection (>20 pixel^2). Actual percentages: No Fascin: 59%, Fascin: 39%, FASNb2: 38%, FASNb5: 50%, No cortactin: 46%, Cortactin: 62%, GELNb11: 62%, CORNb2: 64%. P-values were determined with one way ANOVA (ns non-significant, * $p < 0.05$).

However, some FASNb5-expressing cells completely fail in developing podosomes. Lack of constituents and/or initiation points may be the cause. Indeed, podosomes are believed to arise from focal adhesion disassembly [36] and it was recently reported that fascin-depleted focal adhesions have prolonged lifetime and less dynamics [37]. This may also explain why an assembling role of fascin was suggested before [13], although the broad targeting technique (microRNA) has to be considered also.

Our results are in line with the observation that high fascin levels are responsible for podosome disassembly upon DC maturation [14], which we propose to extend into a more general fascin function in podosome dynamics dependent on its expression levels. In immature DC and THP-1 cells with comparably low fascin levels, bundling inhibition disturbs its regulatory activity in podosome dynamics. Mature DC on the other hand, having high fascin levels, lose the ability to form podosomes [38,39]. The exaggerated fascin bundling potential limits branching to the extent that podosome onset can simply not occur, possibly also by preventing binding of other actin regulators. Lowering fascin levels in mature DC would therefore promote podosome formation [14].

Another fascinating consideration is that fascin actin bundling has a contrasting role in podosomes versus invadopodia. Cancer cells expressing FASNb5 showed reduced invadopodium lifetimes while formation itself was not affected [12]. This may be explained by the different actin arrangements in invadopodia versus podosomes (Fig. 1f). Invadopodia are generated by a dendritic actin network at the base, while elongation occurs upon extension of bundled actin fibers at the tip, partly by fascin [40,11]. As podosomes are less protrusive, they just grow by expanding their branching-based core, with bundling activity controlling on top of the structure [41,4]. Therefore, potent

Fig. 6. Fascin actin bundling and the cortactin SH3 domain regulate degrading and migratory phenotypes in THP-1 macrophages. a. Representative images of parental THP-1 cells with normal or disrupted podosome patterns, seeded for 6 h on a fluorescently labeled gelatin matrix and visualized with vinculin and phalloidin. The disrupted pattern is characterized by disturbed vinculin rings and 'fuzzy' actin centers and is most common in CORNb2-expressing cells as shown in Fig. 2f, g. Scale bar = 10 μm. b. Quantification of degrading parental THP-1 cells with normal or disrupted podosomes as distinguished in a. Bars represent normalized means with SEM (n = 3, 100 cells per repeat). Actual percentages: normal: 87%, disrupted: 26%. c. Representative images of podosome- or focal adhesion type-degradation of a fluorescently labeled gelatin matrix by parental THP-1 cells and visualized by vinculin and phalloidin. Scale bar = 10 μm. d. Quantification of the degradation type as distinguished in c. represented as means with SEM (n = 4, >100 cells per repeat). e. Representative pictures of phalloidin-labeled control or nanobody-expressing cells showing differences in migratory phenotypes. More FASNb5 and CORNb2 cells are rounded and not enriched for podosomes at a particular cell side. Scale bar = 10 μm. f. Boxplot of the circularity index (whiskers from 10 to 90%) of at least 100 cells per condition obtained over 3 independent experiments. Circularity was measured on phalloidin-labeled cells (as represented in e) by means of ImageJ. The index is defined as $4*\pi*(\text{area}/\text{perimeter}^2)$, with a value of 1 indicating a perfect circle. g. Quantification of cells with podosomes localized at a particular cell side and not homogenously or centrally distributed. Phalloidin-labeled cells (as represented in e.) were scored 'positive' when podosomes were enriched at a specific side of the cell. Bars represent normalized means with SEM (n = 3, >100 cells per repeat). Actual percentages: control: 29%, FASNb2: 26%, FASNb5: 20%, CORNb2: 25%. P-values were determined with f. Mann–Whitney U or b, d, and g student T-tests (* $p < 0.05$, ** $p < 0.01$).

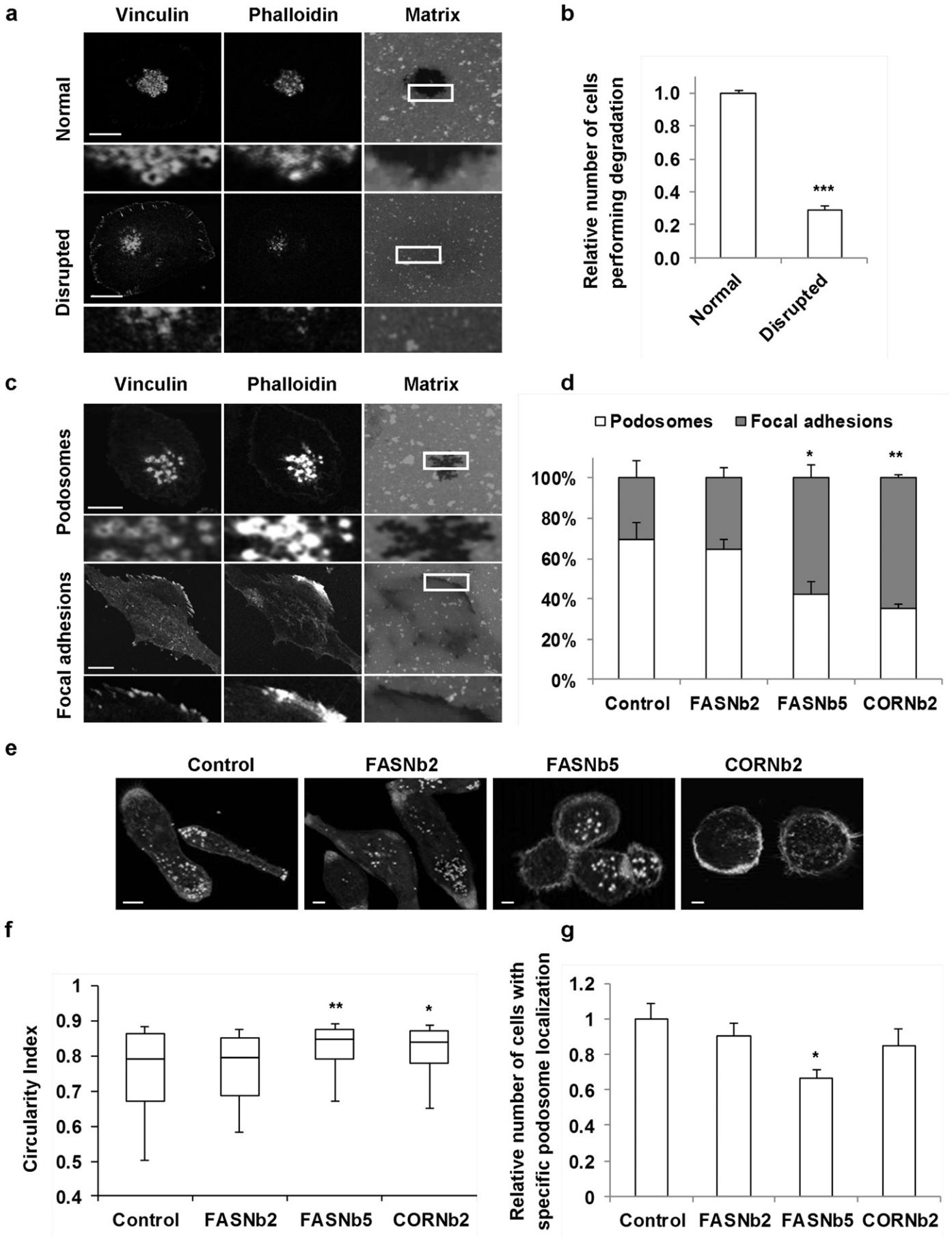
a
Vinculin
Phalloidin
Matrix
Normal
Disrupted
b
Relative number of cells performing degradation
1.0
0.8
0.6
0.4
0.2
0.0
***
Normal
Disrupted
c
Vinculin
Phalloidin
Matrix
Podosomes
Focal adhesions
d
Podosomes
Focal adhesions
100%
80%
60%
40%
20%
0%
*
**
Control
FASNb2
FASNb5
CORNb2
e
Control
FASNb2
FASNb5
CORNb2
f
Circularity Index
1
0.9
0.8
0.7
0.6
0.5
0.4
**
*
Control
FASNb2
FASNb5
CORNb2
g
Relative number of cells with specific podosome localization
1.2
1
0.8
0.6
0.4
0.2
0
*
Control
FASNb2
FASNb5
CORNb2

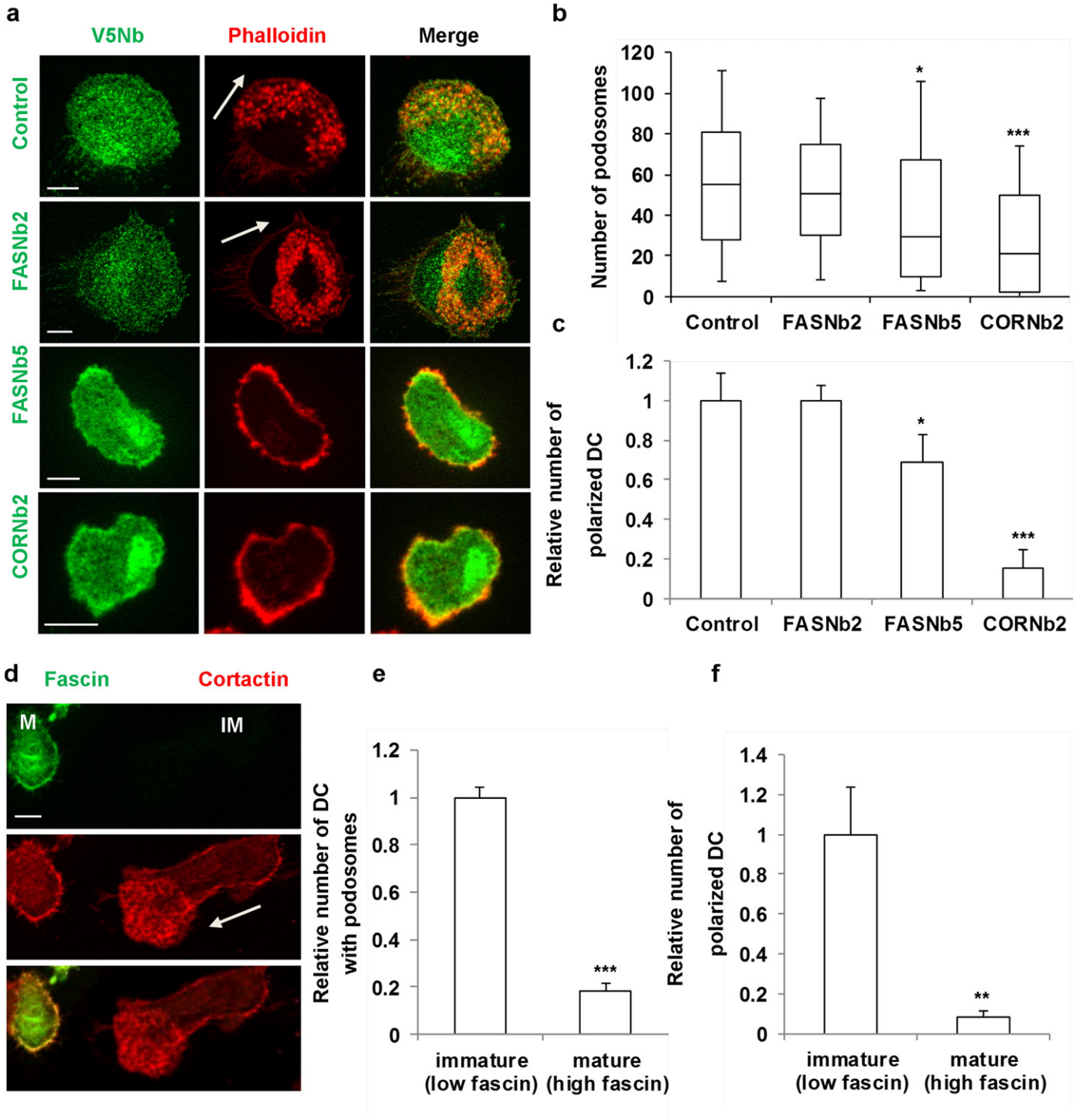

Fig. 7. Fascin actin bundling and the cortactin SH3 domain also mediate podosome formation and a migratory phenotype in primary blood-derived DC. a. Representative pictures of V5-tagged GFPNb (control, anti-GFP nanobody) or fascin/cortactin Nb-transfected DC visualized with anti-V5 antibody and phalloidin. Arrows indicate migratory directions based on cell polarization. Recruitment of podosomes is characteristic for the leading edge, while the trailing edge is devoid of podosomes and often carries filopodia/dendritic protrusions. Scale bar = 10 μm. b. Boxplot of podosome numbers (whiskers from 10–90%) and c. graphs of normalized polarized DC means with SEM as determined in 57–83 cells obtained over 3 independent experiments. Cells were scored 'positive' for polarization when a clear podosome-rich leading edge and a trailing edge devoid of podosomes are present. Cells with no podosomes or equally distributed podosomes along the cell and thus no distinction between leading and trailing edges are scored 'negative'. Actual percentages: control: 54%, FASNb2: 54%, FASNb5: 37%, CORNb2: 8%. d. Representative picture of a mature (M) an immature (IM) DC with the arrow indicating the migratory direction as defined in a. Immunofluorescence of fascin was performed to distinguish mature (high fascin) from immature (low fascin) DC. Cortactin visualizes podosomes. Scale bar = 10 μm. e. Quantification of normalized means (with SEM) of DC with podosomes as determined in 1000 immature and 200 mature DC over 3 independent experiments. Actual percentages: immature: 86%, mature: 16%. f. Quantification of normalized means (with SEM) of polarized DC (as defined in c) as determined in 240 immature and 109 mature DC over 3 independent experiments. Actual percentages: immature: 58%, mature: 4%. Quantification in e and f was done on the basis of images as shown in d, with fascin enabling distinction between mature and immature DC and cortactin enabling podosome visualization. P-values were determined with b Mann–Whitney U or c, e, and f student T-tests (* $p < 0.05$, ** $p < 0.01$, *** $p < 0.001$).

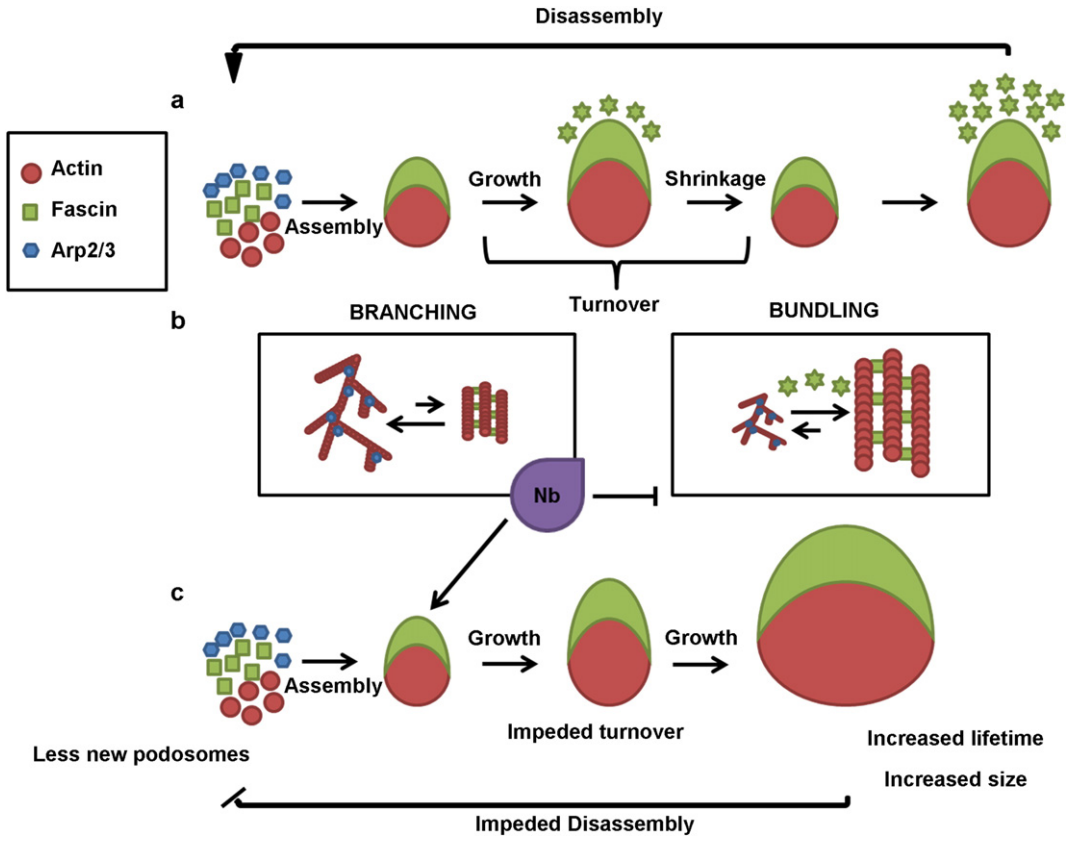

Fig. 8. Scheme of the elucidated role of fascin actin bundling in THP-1 macrophage podosome dynamics by means of a fascin nanobody. a. Podosome life starts with assembly by podosome constituents followed by several rounds of turnover (growth and shrinkage) and finally podosome disassembly delivering constituents for the build-up of new podosomes. Fascin regulates this process from its specific cap-like location by its actin bundling activity (fascin stars). b. While initial assembly and podosome growth occurs due to Arp2/3-dependent actin polymerization, the fascin signal shifts actin modifications from branching towards bundling. This enables shrinkage and final disassembly of the podosome due to loss of branched actin at the tip and formation of bundled actin at the top. c. Due to the bundling-inhibiting capacity of FASNb5, the podosome gets stuck in the 'branching' modus and keeps growing due to the lack of a turnover signal. Therefore, lifetime and size are increased and final disassembly is impeded. This further limits availability of podosome constituents and accounts for reduced podosome numbers.

bundling contributes to invadopodium stability while it regulates turnover and termination of podosomes.

The contribution of bundling proteins (supervillin, formin, …) to podosome disassembly has been suggested before. However, there was no direct link with bundling activity, but rather with interaction partners [42], other actin regulations [43] or phosphorylation [44]. Furthermore, inhibition of L-plastin bundling decreased podosome lifetime and led to structural defects [24]. Thus, fascin bundling-induced podosome disassembly is quite unique. Indeed, L-plastin will rather form bundles onto existing branches [45] and therefore contribute to podosome assembly and stability. Additionally, cofilin may account for the differences as its severing is enhanced in fascin-crosslinks [46], but reduced in bundles generated by formins and villins [47,48].

Altogether our observations point to a unique role of fascin bundling in podosomes of THP-1 macrophages and DC which is mechanistically different from other bundling proteins or other protrusions such as invadopodia.

4.2. Role of the cortactin SH3 domain in podosome assembly and structural integrity

Our results point to a role of the cortactin SH3 domain in podosome assembly. This is in agreement with previous reports on cortactin presence prior to actin at podosome initiation sites [36,49]. As cortactin, lacking a functional SH3 domain, fails in being recruited towards those sites [49], it is likely that CORNb2 affects this initial cluster formation which is the scaffold for actin assembly and thus podosome formation.

Effects on podosome structure integrity were reported previously in HS1 deficient [20] and WIP deficient DC [50,51]. Our results pinpoint this defect to the cortactin SH3 domain. More particular, we showed before that WIP and cortactin recruitment towards the plasma membrane of CORNb2-expressing breast cancer cells was reduced, while DynaminII and WASP remained unaffected [12]. This suggests that disturbed cortactin-WIP recruitment and/or interaction accounts for disrupted podosome structures. This is in agreement with the observation that DC expressing WIP without the cortactin interaction domain also carry disrupted podosomes [50].

The cortactin SH3 domain similarly contributes to assembly and structure in cancer cell invadopodia [12]. However, CORNb2 there also reduced matrix degradation activity. This may be masked in THP-1 cells due to the compensation by proteolytic focal adhesions.

Intriguing is the non-redundant role of cortactin next to HS1 in macrophages and DC. It was shown before that both are expressed in megakaryocytes, platelets and osteoclasts [52–54]. In macrophages and DC however, some report only the presence of HS1 [20,21], while we and others observe expression of both proteins [50,51]. Functionally, HS1 is a weaker actin nucleator and branch mediator compared to cortactin [29]. Furthermore, phosphorylation can occur at different sites, HS1 has a nuclear localization signal while cortactin does not, and their SH3 domain can bind different proteins despite the amino acid similarity of 86% [33]. Thus, our data confirms the idea that cortactin and HS1 expression in myeloid cells is not redundant and that they may be functionally more distinct than assumed. By comparison, hematopoietic WASP and ubiquitous N-WASP are also both necessary in macrophage podosome formation [55].

In conclusion, the cortactin SH3 domain has an assembling role in both invadopodia and podosomes of THP-1 macrophages and DC, independent of the homologue HS1 and most likely involving WIP-cortactin binding.

4.3. Effect of podosome-loss on focal adhesions, matrix degradation and migratory phenotype

For both fascin and cortactin nanobodies, podosome-loss was compensated for by focal adhesions, which are less dynamic [56]. This switch was observed before and is believed to help immune cells in modulating adhesion and migratory potential [51,57]. In our case, the focal adhesions also helped to retain degradation capacity in THP-1 macrophages. Although focal adhesions have long been considered as non-proteolytic, recent data showed their extracellular matrix degradation capacity next to proteolytic invadopodia [58,59]. Our data shows that focal adhesion-dependent degradation can also occur next to podosomal degradation in immune cells (Fig. 6c).

The focal adhesions could however not prevent an effect on migratory phenotype development. Chemotaxis was shown before to be linked to podosomes [8,5], which typically assemble at the leading edge [35]. Thus, both nanobodies might result in impaired migration, although this is more likely for FASNb5, as we also observed reduced podosome translocation towards the cell sides (Fig. 6g).

Thus, both nanobodies affect the adhesive, degrading and migratory phenotype due to podosome-loss.

4.4. Conclusions

In summary, our study revealed the disassembling role of fascin bundling and the assembling role of the cortactin SH3 domain during podosome lifetime in THP-1 macrophages and DC. We discovered the particular cap-like localization of fascin and provided insight into a strikingly opposite role in podosomes versus invadopodia. For cortactin, we unveiled its non-redundant role next to HS1 in THP-1 macrophages and DC. This study further sheds light on the intriguing balance between podosomes and focal adhesions, which may also serve as degrading devices. Our observations therefore contribute to a better understanding of podosome architecture, regulation, dynamics and function in immune cells.

Supplementary data to this article can be found online at http://dx.doi.org/10.1016/j.bbamcr.2015.01.003.

Acknowledgments

We thank Dr. Gholamreza Hassanzadeh Ghassabeh (VIB nanobody service facility, Belgium) for the EGFP nanobody cDNA and Dr. Isabelle Maridonneau Parini (Institut de Pharmacologie et de Biologie Structural, University of Toulouse, France) for the LifeAct–Cherry virus. We thank Dr. Sarah De Clercq and Dr. Aude Guillabert for sharing their experiences on immune cell isolation and manipulation. This work was supported by grants from the Research Foundation Flanders (Fonds Wetenschappelijk Onderzoek (FWO) Vlaanderen, FWO3G022310), Ghent University (BOF13-GOA010) and the Interuniversity Attraction Poles Programme of the Belgian State, Federal Office for Scientific, Technical and Cultural Affairs (IUAP P7/13). I.V.A. is supported by the FWO-Flanders (FWO12/ASP/248).

References

[1] S. Linder, M. Aepfelbacher, Podosomes: adhesion hot-spots of invasive cells, Trends Cell Biol. 13 (7) (2003) 376–385.
[2] D.A. Murphy, S.A. Courtneidge, The 'ins' and 'outs' of podosomes and invadopodia: characteristics, formation and function, Nat. Rev. Mol. Cell Biol. 12 (7) (2011) 413–426. http://dx.doi.org/10.1038/nrm3141.
[3] S. Linder, The matrix corroded: podosomes and invadopodia in extracellular matrix degradation, Trends Cell Biol. 17 (3) (2007) 107–117. http://dx.doi.org/10.1016/j.tcb.2007.01.002.
[4] H. Schachtner, S.D. Calaminus, S.G. Thomas, L.M. Machesky, Podosomes in adhesion, migration, mechanosensing and matrix remodeling, Cytoskeleton 70 (10) (2013) 572–589. http://dx.doi.org/10.1002/cm.21119.
[5] A. Dovas, J.C. Gevrey, A. Grossi, H. Park, W. Abou-Kheir, D. Cox, Regulation of podosome dynamics by WASp phosphorylation: implication in matrix degradation and chemotaxis in macrophages, J. Cell Sci. 122 (Pt 21) (2009) 3873–3882. http://dx.doi.org/10.1242/jcs.051755.
[6] C.V. Carman, P.T. Sage, T.E. Sciuto, M.A. de la Fuente, R.S. Geha, H.D. Ochs, H.F. Dvorak, A.M. Dvorak, T.A. Springer, Transcellular diapedesis is initiated by invasive podosomes, Immunity 26 (6) (2007) 784–797. http://dx.doi.org/10.1016/j.immuni.2007.04.015.
[7] P. Rottiers, F. Saltel, T. Daubon, B. Chaigne-Delalande, V. Tridon, C. Billottet, E. Reuzeau, E. Genot, TGFbeta-induced endothelial podosomes mediate basement membrane collagen degradation in arterial vessels, J. Cell Sci. 122 (Pt 23) (2009) 4311–4318. http://dx.doi.org/10.1242/jcs.057448.
[8] D. Zicha, W.E. Allen, P.M. Brickell, C. Kinnon, G.A. Dunn, G.E. Jones, A.J. Thrasher, Chemotaxis of macrophages is abolished in the Wiskott–Aldrich syndrome, Br. J. Haematol. 101 (4) (1998) 659–665.
[9] Y. Calle, G.E. Jones, C. Jagger, K. Fuller, M.P. Blundell, J. Chow, T. Chambers, A.J. Thrasher, WASp deficiency in mice results in failure to form osteoclast sealing zones and defects in bone resorption, Blood 103 (9) (2004) 3552–3561. http://dx.doi.org/10.1182/blood-2003-04-1259.
[10] L. Chen, S. Yang, J. Jakoncic, J.J. Zhang, X.Y. Huang, Migrastatin analogues target fascin to block tumour metastasis, Nature 464 (7291) (2010) 1062–1066. http://dx.doi.org/10.1038/nature08978.
[11] A. Li, J.C. Dawson, M. Forero-Vargas, H.J. Spence, X. Yu, I. Konig, K. Anderson, L.M. Machesky, The actin-bundling protein fascin stabilizes actin in invadopodia and potentiates protrusive invasion, Curr. Biol. 20 (4) (2010) 339–345. http://dx.doi.org/10.1016/j.cub.2009.12.035.
[12] I. Van Audenhove, C. Boucherie, L. Pieters, O. Zwaenepoel, B. Vanloo, E. Martens, C. Verbrugge, G. Hassanzadeh-Ghassabeh, J. Vandekerckhove, M. Cornelissen, A. De Ganck, J. Gettemans, Stratifying fascin and cortactin function in invadopodium formation using inhibitory nanobodies and targeted subcellular delocalization, FASEB J. 28 (4) (2014) 1805–1818. http://dx.doi.org/10.1096/fj.13-242537.
[13] M. Quintavalle, L. Elia, G. Condorelli, S.A. Courtneidge, MicroRNA control of podosome formation in vascular smooth muscle cells in vivo and in vitro, J. Cell Biol. 189 (1) (2010) 13–22. http://dx.doi.org/10.1083/jcb.200912096.
[14] Y. Yamakita, F. Matsumura, M.W. Lipscomb, P.C. Chou, G. Werlen, J.K. Burkhardt, S. Yamashiro, Fascin1 promotes cell migration of mature dendritic cells, J. Immunol. 186 (5) (2011) 2850–2859. http://dx.doi.org/10.4049/jimmunol.1001667.
[15] R. Ross, H. Jonuleit, M. Bros, X.L. Ross, S. Yamashiro, F. Matsumura, A.H. Enk, J. Knop, A.B. Reske-Kunz, Expression of the actin-bundling protein fascin in cultured human dendritic cells correlates with dendritic morphology and cell differentiation, J. Invest. Dermatol. 115 (4) (2000) 658–663. http://dx.doi.org/10.1046/j.1523-1747.2000.00112.x.
[16] M.M. Al-Alwan, G. Rowden, T.D. Lee, K.A. West, Fascin is involved in the antigen presentation activity of mature dendritic cells, J. Immunol. 166 (1) (2001) 338–345.
[17] K.C. Kirkbride, B.H. Sung, S. Sinha, A.M. Weaver, Cortactin: a multifunctional regulator of cellular invasiveness, Cell Adhes. Migr. 5 (2) (2011) 187–198.
[18] M. Oser, H. Yamaguchi, C.C. Mader, J.J. Bravo-Cordero, M. Arias, X. Chen, V. Desmarais, J. van Rheenen, A.J. Koleske, J. Condeelis, Cortactin regulates cofilin and N-WASp activities to control the stages of invadopodium assembly and maturation, J. Cell Biol. 186 (4) (2009) 571–587. http://dx.doi.org/10.1083/jcb.200812176.
[19] E.S. Clark, A.M. Weaver, A new role for cortactin in invadopodia: regulation of protease secretion, Eur. J. Cell Biol. 87 (8–9) (2008) 581–590. http://dx.doi.org/10.1016/j.ejcb.2008.01.008.
[20] D.A. Dehring, F. Clarke, B.G. Ricart, Y. Huang, T.S. Gomez, E.K. Williamson, D.A. Hammer, D.D. Billadeau, Y. Argon, J.K. Burkhardt, Hematopoietic lineage cell-specific protein 1 functions in concert with the Wiskott–Aldrich syndrome protein to promote podosome array organization and chemotaxis in dendritic cells, J. Immunol. 186 (8) (2011) 4805–4818. http://dx.doi.org/10.4049/jimmunol.1003102.
[21] Y. Huang, C. Biswas, D.A. Klos Dehring, U. Sriram, E.K. Williamson, S. Li, F. Clarke, S. Gallucci, Y. Argon, J.K. Burkhardt, The actin regulatory protein HS1 is required for antigen uptake and presentation by dendritic cells, J. Immunol. 187 (11) (2011) 5952–5963. http://dx.doi.org/10.4049/jimmunol.1100870.
[22] C. Hamers-Casterman, T. Atarhouch, S. Muyldermans, G. Robinson, C. Hamers, E.B. Songa, N. Bendahman, R. Hamers, Naturally occurring antibodies devoid of light chains, Nature 363 (6428) (1993) 446–448. http://dx.doi.org/10.1038/363446a0.
[23] G. Hassanzadeh-Ghassabeh, N. Devoogdt, P. De Pauw, C. Vincke, S. Muyldermans, Nanobodies and their potential applications, Nanomedicine 8 (6) (2013) 1013–1026. http://dx.doi.org/10.2217/nnm.13.86.
[24] S. De Clercq, C. Boucherie, J. Vandekerckhove, J. Gettemans, A. Guillabert, L-plastin nanobodies perturb matrix degradation, podosome formation, stability and lifetime in THP-1 macrophages, PLoS One 8 (11) (2013) e78108. http://dx.doi.org/10.1371/journal.pone.0078108.
[25] S. De Clercq, O. Zwaenepoel, E. Martens, J. Vandekerckhove, A. Guillabert, J. Gettemans, Nanobody-induced perturbation of LFA-1/L-plastin phosphorylation impairs MTOC docking, immune synapse formation and T cell activation, Cell. Mol. Life Sci. 70 (5) (2013) 909–922. http://dx.doi.org/10.1007/s00018-012-1169-0.

[26] K. Van Impe, J. Bethuyne, S. Cool, F. Impens, D. Ruano-Gallego, O. De Wever, B. Vanloo, M. Van Troys, K. Lambein, C. Boucherie, E. Martens, O. Zwaenepoel, G. Hassanzadeh-Ghassabeh, J. Vandekerckhove, K. Gevaert, L.A. Fernandez, N.N. Sanders, J. Gettemans, A nanobody targeting the F-actin capping protein CapG restrains breast cancer metastasis, Breast Cancer Res. BCR 15 (6) (2013) R116. http://dx.doi.org/10.1186/bcr3585.
[27] I. Van Audenhove, K. Van Impe, D. Ruano-Gallego, S. De Clercq, K. De Muynck, B. Vanloo, H. Verstraete, L.A. Fernandez, J. Gettemans, Mapping cytoskeletal protein function in cells by means of nanobodies, Cytoskeleton 70 (10) (2013) 604–622. http://dx.doi.org/10.1002/cm.21122.
[28] S.J. Park, S. Suetsugu, H. Sagara, T. Takenawa, HSP90 cross-links branched actin filaments induced by N-WASP and the Arp2/3 complex, Genes Cells 12 (5) (2007) 611–622. http://dx.doi.org/10.1111/j.1365-2443.2007.01081.x.
[29] T. Uruno, P. Zhang, J. Liu, J.J. Hao, X. Zhan, Haematopoietic lineage cell-specific protein 1 (HS1) promotes actin-related protein (Arp) 2/3 complex-mediated actin polymerization, Biochem. J. 371 (Pt 2) (2003) 485–493. http://dx.doi.org/10.1042/BJ20021791.
[30] A. Van den Abbeele, S. De Clercq, A. De Ganck, V. De Corte, B. Van Loo, S.H. Soror, V. Srinivasan, J. Steyaert, J. Vandekerckhove, J. Gettemans, A llama-derived gelsolin single-domain antibody blocks gelsolin-G-actin interaction, Cell. Mol. Life Sci. 67 (9) (2010) 1519–1535. http://dx.doi.org/10.1007/s00018-010-0266-1.
[31] J. Auwerx, The human leukemia cell line, THP-1: a multifacetted model for the study of monocyte-macrophage differentiation, Experientia 47 (1) (1991) 22–31.
[32] S. Tsuchiya, Y. Kobayashi, Y. Goto, H. Okumura, S. Nakae, T. Konno, K. Tada, Induction of maturation in cultured human monocytic leukemia cells by a phorbol diester, Cancer Res. 42 (4) (1982) 1530–1536.
[33] A.G. van Rossum, E. Schuuring-Scholtes, Seggelen V. van Buuren-van, P.M. Kluin, E. Schuuring, Comparative genome analysis of cortactin and HS1: the significance of the F-actin binding repeat domain, BMC Genomics 6 (2005) 15. http://dx.doi.org/10.1186/1471-2164-6-15.
[34] O. Destaing, F. Saltel, J.C. Geminard, P. Jurdic, F. Bard, Podosomes display actin turnover and dynamic self-organization in osteoclasts expressing actin-green fluorescent protein, Mol. Biol. Cell 14 (2) (2003) 407–416. http://dx.doi.org/10.1091/mbc.E02-07-0389.
[35] J.G. Evans, I. Correia, O. Krasavina, N. Watson, P. Matsudaira, Macrophage podosomes assemble at the leading lamella by growth and fragmentation, J. Cell Biol. 161 (4) (2003) 697–705. http://dx.doi.org/10.1083/jcb.200212037.
[36] I. Kaverina, T.E. Stradal, M. Gimona, Podosome formation in cultured A7r5 vascular smooth muscle cells requires Arp2/3-dependent de-novo actin polymerization at discrete microdomains, J. Cell Sci. 116 (Pt 24) (2003) 4915–4924. http://dx.doi.org/10.1242/jcs.00818.
[37] N. Elkhatib, M.B. Neu, C. Zensen, K.M. Schmoller, D. Louvard, A.R. Bausch, T. Betz, D.M. Vignjevic, Fascin plays a role in stress fiber organization and focal adhesion disassembly, Curr. Biol. 24 (13) (2014) 1492–1499. http://dx.doi.org/10.1016/j.cub.2014.05.023.
[38] S. Burns, S.J. Hardy, J. Buddle, K.L. Yong, G.E. Jones, A.J. Thrasher, Maturation of DC is associated with changes in motile characteristics and adherence, Cell Motil. Cytoskeleton 57 (2) (2004) 118–132. http://dx.doi.org/10.1002/cm.10163.
[39] M.A. West, R.P. Wallin, S.P. Matthews, H.G. Svensson, R. Zaru, H.G. Ljunggren, A.R. Prescott, C. Watts, Enhanced dendritic cell antigen capture via toll-like receptor-induced actin remodeling, Science 305 (5687) (2004) 1153–1157. http://dx.doi.org/10.1126/science.1099153.
[40] M. Schoumacher, R.D. Goldman, D. Louvard, D.M. Vignjevic, Actin, microtubules, and vimentin intermediate filaments cooperate for elongation of invadopodia, J. Cell Biol. 189 (3) (2010) 541–556. http://dx.doi.org/10.1083/jcb.200909113.
[41] S. Linder, C. Wiesner, M. Himmel, Degrading devices: invadosomes in proteolytic cell invasion, Annu. Rev. Cell Dev. Biol. 27 (2011) 185–211. http://dx.doi.org/10.1146/annurev-cellbio-092910-154216.
[42] R. Bhuwania, S. Cornfine, Z. Fang, M. Kruger, E.J. Luna, S. Linder, Supervillin couples myosin-dependent contractility to podosomes and enables their turnover, J. Cell Sci. 125 (Pt 9) (2012) 2300–2314. http://dx.doi.org/10.1242/jcs.100032.
[43] A.T. Mersich, M.R. Miller, H. Chkourko, S.D. Blystone, The formin FRL1 (FMNL1) is an essential component of macrophage podosomes, Cytoskeleton 67 (9) (2010) 573–585. http://dx.doi.org/10.1002/cm.20468.
[44] A. Dorfleutner, Y. Cho, D. Vincent, J. Cunnick, H. Lin, S.A. Weed, C. Stehlik, D.C. Flynn, Phosphorylation of AFAP-110 affects podosome lifespan in A7r5 cells, J. Cell Sci. 121 (Pt 14) (2008) 2394–2405. http://dx.doi.org/10.1242/jcs.026187.
[45] C.T. Skau, D.S. Courson, A.J. Bestul, J.D. Winkelman, R.S. Rock, V. Sirotkin, D.R. Kovar, Actin filament bundling by fimbrin is important for endocytosis, cytokinesis, and polarization in fission yeast, J. Biol. Chem. 286 (30) (2011) 26964–26977. http://dx.doi.org/10.1074/jbc.M111.239004.
[46] D. Breitsprecher, S.A. Koestler, I. Chizhov, M. Nemethova, J. Mueller, B.L. Goode, J.V. Small, K. Rottner, J. Faix, Cofilin cooperates with fascin to disassemble filopodial actin filaments, J. Cell Sci. 124 (Pt 19) (2011) 3305–3318. http://dx.doi.org/10.1242/jcs.086934.
[47] A. Michelot, J. Berro, C. Guerin, R. Boujemaa-Paterski, C.J. Staiger, J.L. Martiel, L. Blanchoin, Actin-filament stochastic dynamics mediated by ADF/cofilin, Curr. Biol. 17 (10) (2007) 825–833. http://dx.doi.org/10.1016/j.cub.2007.04.037.
[48] S. Huang, R.C. Robinson, L.Y. Gao, T. Matsumoto, A. Brunet, L. Blanchoin, C.J. Staiger, Arabidopsis VILLIN1 generates actin filament cables that are resistant to depolymerization, Plant Cell 17 (2) (2005) 486–501. http://dx.doi.org/10.1105/tpc.104.028555.
[49] B.A. Webb, R. Eves, A.S. Mak, Cortactin regulates podosome formation: roles of the protein interaction domains, Exp. Cell Res. 312 (6) (2006) 760–769. http://dx.doi.org/10.1016/j.yexcr.2005.11.032.
[50] I. Banon-Rodriguez, J. Monypenny, C. Ragazzini, A. Franco, Y. Calle, G.E. Jones, I.M. Anton, The cortactin-binding domain of WIP is essential for podosome formation and extracellular matrix degradation by murine dendritic cells, Eur. J. Cell Biol. 90 (2–3) (2011) 213–223. http://dx.doi.org/10.1016/j.ejcb.2010.09.001.
[51] H.C. Chou, I.M. Anton, M.R. Holt, C. Curcio, S. Lanzardo, A. Worth, S. Burns, A.J. Thrasher, G.E. Jones, Y. Calle, WIP regulates the stability and localization of WASP to podosomes in migrating dendritic cells, Curr. Biol. 16 (23) (2006) 2337–2344. http://dx.doi.org/10.1016/j.cub.2006.10.037.
[52] X. Zhan, C.C. Haudenschild, Y. Ni, E. Smith, C. Huang, Upregulation of cortactin expression during the maturation of megakaryocytes, Blood 89 (2) (1997) 457–464.
[53] S.G. Thomas, S.D. Calaminus, J.M. Auger, S.P. Watson, L.M. Machesky, Studies on the actin-binding protein HS1 in platelets, BMC Cell Biol. 8 (2007) 46. http://dx.doi.org/10.1186/1471-2121-8-46.
[54] S. Tehrani, R. Faccio, I. Chandrasekar, F.P. Ross, J.A. Cooper, Cortactin has an essential and specific role in osteoclast actin assembly, Mol. Biol. Cell 17 (7) (2006) 2882–2895. http://dx.doi.org/10.1091/mbc.E06-03-0187.
[55] L.M. Nusblat, A. Dovas, D. Cox, The non-redundant role of N-WASP in podosome-mediated matrix degradation in macrophages, Eur. J. Cell Biol. 90 (2–3) (2011) 205–212. http://dx.doi.org/10.1016/j.ejcb.2010.07.012.
[56] R.M. Saunders, M.R. Holt, L. Jennings, D.H. Sutton, I.L. Barsukov, A. Bobkov, R.C. Liddington, E.A. Adamson, G.A. Dunn, D.R. Critchley, Role of vinculin in regulating focal adhesion turnover, Eur. J. Cell Biol. 85 (6) (2006) 487–500. http://dx.doi.org/10.1016/j.ejcb.2006.01.014.
[57] M.A. West, A.R. Prescott, K.M. Chan, Z. Zhou, S. Rose-John, J. Scheller, C. Watts, TLR ligand-induced podosome disassembly in dendritic cells is ADAM17 dependent, J. Cell Biol. 182 (5) (2008) 993–1005. http://dx.doi.org/10.1083/jcb.200801022.
[58] Y. Wang, M.A. McNiven, Invasive matrix degradation at focal adhesions occurs via protease recruitment by a FAK-p130Cas complex, J. Cell Biol. 196 (3) (2012) 375–385. http://dx.doi.org/10.1083/jcb.201105153.
[59] H. Tang, A. Li, J. Bi, D.M. Veltman, T. Zech, H.J. Spence, X. Yu, P. Timpson, R.H. Insall, M.C. Frame, L.M. Machesky, Loss of Scar/WAVE complex promotes N-WASP- and FAK-dependent invasion, Curr. Biol. 23 (2) (2013) 107–117. http://dx.doi.org/10.1016/j.cub.2012.11.059.